

Facile and Label-Free Detection of Lung Cancer Biomarker in Urine by Magnetically Assisted Surface-Enhanced Raman Scattering

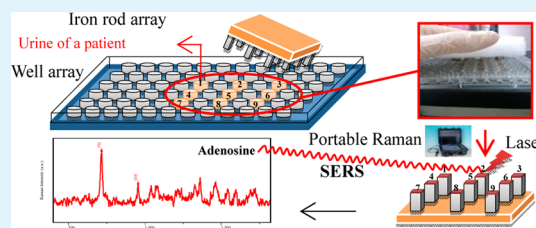
Tianxi Yang, Xiaoyu Guo, Yiping Wu, Hui Wang, Shuyue Fu, Ying Wen, and Haifeng Yang*

The Education Ministry Key Lab of Resource Chemistry, Shanghai Key Laboratory of Rare Earth Functional Materials, Shanghai Municipal Education Committee Key Laboratory of Molecular Imaging Probes and Sensors and Department of Chemistry, Shanghai Normal University, Shanghai 200234, P. R. China

Supporting Information

ABSTRACT: Adenosine plays a crucial role in the regulation of physiological activity in various tissues and organs. As adenosine is a possible biomarker for cancer, the determination of its level presents a demanding task for deeply monitoring progress of diseases. Through the synthesis of $\text{Fe}_3\text{O}_4/\text{Au}/\text{Ag}$ nanocomposites weaved and stabilized by phytic acid and its salt, we develop a magnetically assisted surface-enhanced Raman scattering (SERS) protocol to determine trace level adenosine in urine samples from both lung cancer patients and health human. The magnetic properties of the nanocomposites enable to realize the simple separation of targeted molecules from a complex matrix and the Au/Ag nanoparticles moieties act as the SERS platform. This label-free $\text{Fe}_3\text{O}_4/\text{Au}/\text{Ag}$ -nanocomposites-based SERS protocol shows a good stability, reproducibility, time efficiency (less than 20 min for one sample test), and huge sensitivity down to 1×10^{-10} M. The protocol also has high selectivity because SERS signal of adenosine provides the molecular fingerprint information as well as an azo coupling pretreatment is performed to remove the interference of urea. Furthermore, a SERS array is designed for on-site screening adenosine in urine samples in a massive way using a portable Raman. Such a magnetically assisted SERS method as a powerful alternative can be expected as a smart and promising tool for effective assessment of healthcare.

KEYWORDS: $\text{Fe}_3\text{O}_4/\text{Au}/\text{Ag}$ nanocomposites, SERS, adenosine, cancer biomarker, urine, azo coupling



INTRODUCTION

Adenosine as an important endogenous modulator plays a vital role in the regulation of physiological activity in various tissues and organs.¹ It has been reported that the rapid growth of solid tumors conventionally experiences severe hypoxia and necrosis, resulting in degradation of adenosine nucleotide to release adenosine. The released adenosine would accumulate in solid tumors at high concentrations, which may benefit malignancy by providing a supportive environment.² Therefore, adenosine has been considered as a possible biomarker for cancer, and also used for monitoring progress of diseases.³ Furthermore, directly monitoring of adenosine fluctuations under physiological conditions in body fluids, would also plays a key role in the investigation of brain function and behavior.⁴

Urine is convenient to collected and pretreat and less interference from urine is beneficial for the detection of trace adenosine. The determination of urinary adenosine is usually performed using high-performance liquid chromatography (HPLC)^{5,6} and gas chromatography–mass spectrometry (GC-MS).⁷ Although HPLC coupled with fluorescence detection allows sensitive and selective analysis of adenosine, most of them require expensive instruments, time-consuming sample pretreatment, and fluorescence derivatization steps. GC-MS method is highly effective but the requirement of a mass spectrometer makes it unavailable for routinely on-field monitoring. There is an increasing demand for developing a

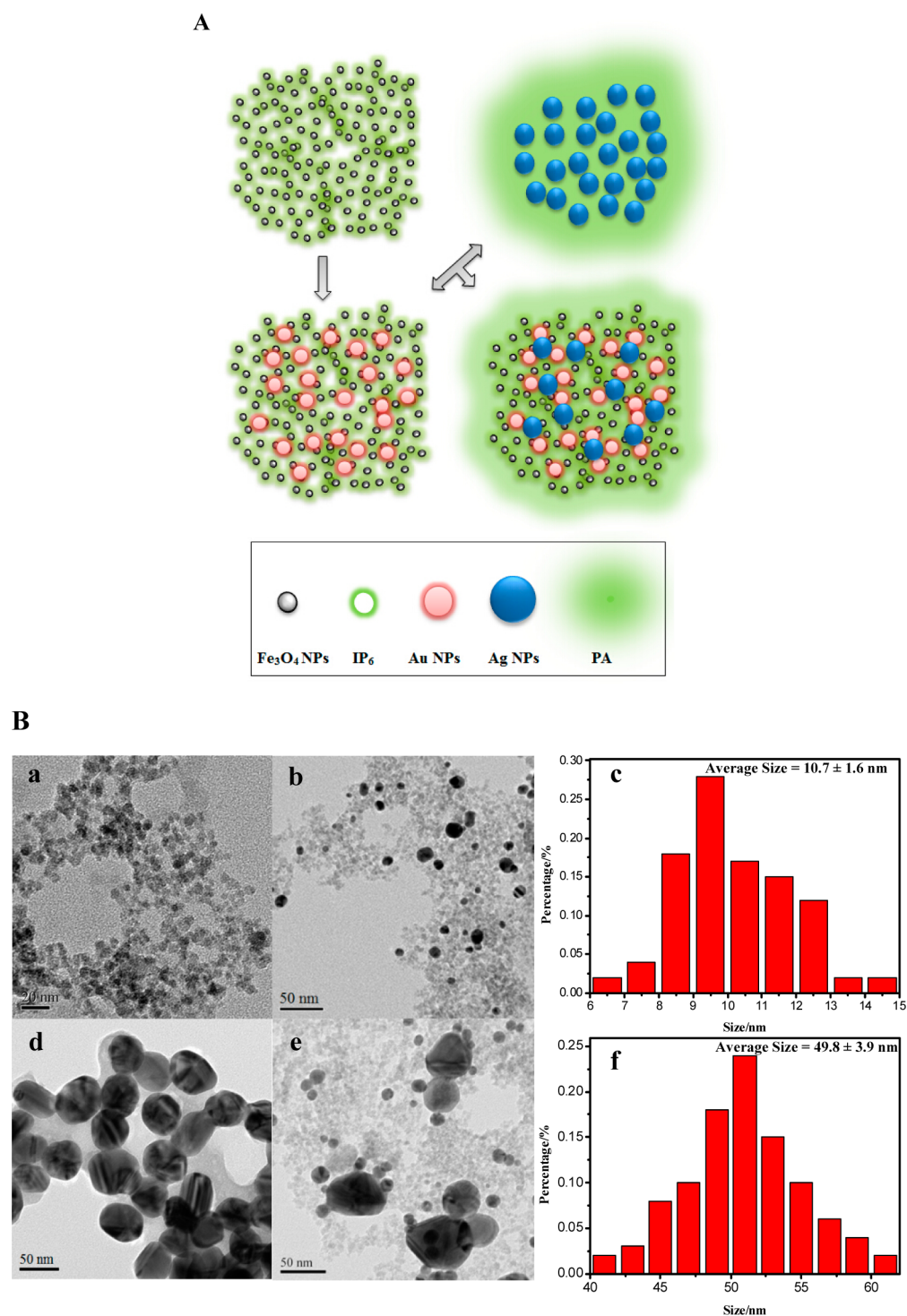
simple, sensitive and selective method to determine adenosine in human urine. For the merit of easy operation and reliability of the molecular information, Raman spectroscopic analysis of adenosine can be an alternative method. Notably, because of the huge sensitivity of surface-enhanced Raman scattering (SERS),^{8–11} it could be available to analyze the physiological levels of adenosine in urine. In recent years, SERS methods were developed for measuring adenosine based on aptamer technique.^{12–14} Compared with aptamer-based approach, label-free methods may be cheaper, easier to operate, and time efficient. So far, there is no related literature reported about label-free SERS detection of urinary adenosine.

The SERS technique usually utilizes noble metals (Au and Ag, etc.) at the nanosize level.^{15,16} The selectivity of SERS method can be further increased by surface modification of respective nanoparticles.^{17,18} Moreover, for SERS measurement as a rapid method, the simplification and time efficiency for sample pretreatment are demanded. However, SERS analysis of samples in a matrix presenting a highly complex system is confronted with a challenge. Therefore, the construction of SERS-active substrate with magnetic properties is one of the available ways.^{19–21} The ability of magnetically separating the

Received: August 26, 2014

Accepted: November 13, 2014

Published: November 13, 2014



target from the complex matrix and magnetic effect assisted to improve the detection sensitivity of SERS measurement. In our previous work,²² $\text{Fe}_3\text{O}_4/\text{Au}$ nanocomposites were successfully prepared to on-site monitor trace pesticide at vegetable peels with a portable Raman system. $\text{Fe}_3\text{O}_4/\text{Au}$ -nanocomposites-based SERS method was tentatively employed to determine the adenosine in urine and the reasonable Raman signal of trace adenosine in urine was failed to be observed.

In this work, we present an improved SERS method for the analysis of adenosine in human urine through synthesis of $\text{Fe}_3\text{O}_4/\text{Au}/\text{Ag}$ nanocomposites with the help of phytic acid and its sodium salt. The $\text{Fe}_3\text{O}_4/\text{Au}/\text{Ag}$ nanocomposites-based SERS protocol with high sensitivity and reproducibility can be successfully applied to detect adenosine in urine from lung cancer patient with a portable Raman spectrometer. Compared to the chromatographic approaches, the present method has

considerable time efficiency (less than 20 min for a sample), selectivity and reliability. Furthermore, the $\text{Fe}_3\text{O}_4/\text{Au}/\text{Ag}$ nanocomposite-based SERS method is designed to require low sample volumes at microliter level, because a magnetic extraction procedure allows easy separation of the target analyte from the matrix to avoid interference to some extent. Additionally, azo coupling reaction is conducted to remove negative effect of urea on the SERS detection of adenosine. Finally, a SERS array is also designed to detect the urine sample of lung cancer patients in high throughput. As a perspective, this proposed SERS method is potentially applicable in a clinical and diagnostic praxis performed on human models.

EXPERIMENTAL SECTION

Materials. Sodium salt of phytic acid (IP_6 , 90%) and phytic acid (PA, 50 wt %) solution were purchased from Sigma-Aldrich. $\text{FeCl}_3 \cdot 6\text{H}_2\text{O}$ (99%), $\text{FeCl}_2 \cdot 4\text{H}_2\text{O}$ (99%), NaOH ($\geq 96.0\%$), sodium citrate ($\text{Na}_3\text{C}_6\text{H}_5\text{O}_7 \cdot 2\text{H}_2\text{O}$, 99.8%), chloroauric acid ($\text{HAuCl}_4 \cdot 4\text{H}_2\text{O}$, 99.9%), Rhodamine 6G (R6G), adenosine, guanosine, cytidine, uridine, thymidine, and urea were used without further purification. Ultrapure water (18 $\text{M}\Omega \text{ cm}$) was produced using a Millipore water purification system and used for all solution preparations.

Instruments. The morphologies of nanocomposites were measured with a JEOL JEM-2000 FX transmission electron microscopy (TEM) operating at 200 kV. X-ray photoelectron spectroscopy (XPS; PHI 5000 Versa Probe) was performed to identify the chemical composition of the surface of the observed nanocomposites. The metal amount in nanocomposites was determined with inductively coupled plasma-atomic emission spectroscopy (ICP-AES) (Varian VISTA-MPX). HPLC-MS experiment was conducted with HPLC analyzer (Agilent 6410 series Triple Quad). A Jobin Yvon micro-Raman spectroscope (Super LabRam II) with a mode of 50 \times objective (8 mm), a holographic grating (1800 g mm^{-1}), 1024 \times 256 pixels charge-coupled device detector and 5 mW He-Ne laser at 632.8 nm as an excitation line was employed for Raman measurements. A Portable Stabilized R. Laser Analyzer (Enwave) with a narrow line width diode laser at 785 nm with an adjustable power of the maximum at 300 mW was also used for online detection purpose.

Preparation of $\text{Fe}_3\text{O}_4/\text{Au}/\text{Ag}$ Nanocomposites. Fe_3O_4 nanoparticles (NPs) were made via the chemical coprecipitation method in the presence of IP_6 following a reported method.²² The product of magnetic NPs protected by IP_6 was black brown. The Fe_3O_4 NPs were rinsed multiple times with ultrapure water and collected from the solution by applying an external magnetic field. Then, it was dissolved in 10 mL of water for Au modification. In brief, 10 mL of the collected magnetic NPs (0.76 mg mL^{-1}) was dispersed in 150 mL of ultrapure water and then heated to boiling. After slowly injecting 5 mL of 1% chloroauric acid under vigorous stirring, the mixed solution was refluxed for 15 min and 5 mL of 1% sodium citrate was rapidly added into the solution. The final color of mixture presented reddish brown after heating for additional 45 min. The mixture was cooled to room temperature and the resulting NPs were collected by a magnet and washed several times with ultrapure water. The preparation of $\text{Fe}_3\text{O}_4/\text{Au}/\text{Ag}$ nanocomposites was as follows: first, the Ag NPs were prepared by a method which was similar to Lee's method excepting the presence of PA. Briefly, 0.0255 g of AgNO_3 was dissolved in 150 mL of ultrapure water in the flask. Then 5 mL of 0.001 M PA solution was added into the above solution. After that, the solution was heated to boiling before 3 mL of 1% sodium citrate solution was added slowly under vigorous stirring. The mixed solution was heating for additional 30 min and cooled to room temperature. The product was centrifuged and washed with ultrapure water twice. Then, it was dissolved in 10 mL of ultrapure water and used for fabrication of $\text{Fe}_3\text{O}_4/\text{Au}/\text{Ag}$ nanocomposites. Forty milliliters of 0.29 mg mL^{-1} $\text{Fe}_3\text{O}_4/\text{Au}$ nanocomposites were mixed with 0.18 mg mL^{-1} Ag NPs and the mixture kept boiling for 30 min under vigorous stirring. The volume of 0.18 mg mL^{-1} Ag NPs changed from 1 to 4 mL, whereas the content of $\text{Fe}_3\text{O}_4/\text{Au}$ nanocomposites kept constant, resulting in the increase

in Ag NPs onto the surface of $\text{Fe}_3\text{O}_4/\text{Au}$ nanocomposites. The obtained precipitates were rinsed multiple times with ultrapure water and collected from the solution by an external magnet.

Preparation of Urine Samples. The healthy urine was obtained from disease-free volunteers. Approximately 100 mL of urine was collected and aliquots of the urine were spiked with different concentrations of adenosine. Each simulated sample was allowed to equilibrate for 30 min at room temperature prior to SERS experiment. Freshly voided urine samples were obtained from some preoperation patients with lung cancer, which were from Shanghai Pulmonary Hospital. The prepared urine samples were centrifuged for 10 min at 10000 rpm to remove particulate matter.

Raman Measurements for the Samples. In the case of Raman spectrum recorded with micro-Raman spectroscope, the acquisition time for each sample at typically 8 s and three accumulations were set. For online detection, the laser power of the Portable Raman Analyzer was used of 300 mW, the acquisition time in each case was 1 s and five accumulations.

High Performance Liquid Chromatography Tandem Mass Spectrometry. The human urine samples were also analyzed on Agilent 6410 series Triple Quad HPLC equipped with an UV-detector. The analytical column was Agilent C18 column, maintained at 30 $^\circ\text{C}$. A binary gradient consisting of 90% 5 mM ammonium acetate, pH 5.0, and 10% methanol was used for HPLC analysis at a rate of 0.8 mL/min. The injection volume was 5 μL . A microsplitter valve (Agilent Technologies, Palo Alto, CA) delivered 50% of the flow to the mass spectrometer. Capillary voltage was set at 3500 V. High purity nitrogen (99.999%) was used as collision gas. Ion source temperature was 300 $^\circ\text{C}$, with nitrogen for nebulization and desolvation. Chromatograms were obtained in the positive ion and multiple reactions monitoring mode (ESI^+ -MRM).

RESULTS AND DISCUSSION

Characterization of $\text{Fe}_3\text{O}_4/\text{Au}/\text{Ag}$ Nanocomposites.

The determination of adenosine in human urine presents a relatively important task since adenosine plays a significant role in regulation of physiological activity. Herein, we developed the $\text{Fe}_3\text{O}_4/\text{Au}/\text{Ag}$ nanocomposite-SERS method for the direct and selective detection of trace adenosine in urine. As a magnetic SERS substrate, the nanocomposites could also separate the targeted adenosine from a matrix of urine with magnetic force. The synthesis strategy of $\text{Fe}_3\text{O}_4/\text{Au}/\text{Ag}$ nanocomposites is shown in Figure 1A. In brief, Fe_3O_4 NPs are synthesized using the chemical coprecipitation approach and stabilized by IP_6 (Figure 1B-a). Second, Au NPs are formed on the surface of Fe_3O_4 NPs using 5 mL of 1% HAuCl_4 as gold precursor and 10 mL of 1% sodium citrate as a reducing agent. The average size of Au NPs is 10.7 ± 1.6 nm, estimated by TEM results (Figure 1B-b, c). To remove free Au nanoparticles, these composite nanoparticles are magnetically isolated using an external magnet. Next, in the presence of PA as a stabilizer and a bridging agent, Ag NPs are prepared using AgNO_3 and sodium citrate (Figure 1B-d). Figure 1B-f shows the average size of Ag NPs is 49.8 ± 3.9 nm. Mixing the $\text{Fe}_3\text{O}_4/\text{Au}$ with PA-covered Ag NPs can facilely form the nanocomposites of $\text{Fe}_3\text{O}_4/\text{Au}/\text{Ag}$ (Figure 1B-e). The growth mechanism of $\text{Fe}_3\text{O}_4/\text{Au}/\text{Ag}$ nanocomposites is described as follows: Fe_3O_4 protected and linked by IP_6 were dotted with Au NPs to form $\text{Fe}_3\text{O}_4/\text{Au}$ nanocomposites. $\text{Fe}_3\text{O}_4/\text{Au}$ nanocomposites could further bind the PA/Ag NPs through free phosphates chelating nanoparticles to form the final product, shortly named as $\text{Fe}_3\text{O}_4/\text{Au}/\text{Ag}$ nanocomposites. In Figure S1-a in the Supporting Information, HR-TEM image of $\text{IP}_6/\text{Fe}_3\text{O}_4$ nanocomposites shows the average particle size of Fe_3O_4 NPs about 5 nm (d -spacing of Fe_3O_4 NPs is 0.262 nm, corresponding to the Fe (311) plane). Clearly, Fe_3O_4 NPs are weaved by IP_6 to form the

net structure. Figure S1-b in the Supporting Information is TEM image of $\text{Fe}_3\text{O}_4/\text{Au}/\text{Ag}$ nanocomposites with larger scale, which could be seen that the Ag NPs and Au NPs are tightly dotted onto the Fe_3O_4 nanocomposites. In the structure of $\text{Fe}_3\text{O}_4/\text{Au}/\text{Ag}$ nanocomposites, there are many junctions between Au NPs (small size) and Ag NPs (big size), which was beneficial to producing huge Raman enhancement.²³ XPS method was employed to provide elemental information.²⁴ XPS results (see Figure S2 in the Supporting Information) of the $\text{Fe}_3\text{O}_4/\text{Au}/\text{Ag}$ nanocomposites indicate the compositions of Fe, Au, Ag, and P.

UV-visible spectrum of $\text{Fe}_3\text{O}_4/\text{Au}$ nanocomposites presents a SPR peak at ~ 525 nm (see Figure S3A-d in the Supporting Information), which is slightly red-shifted compared to the band at 520 nm from free Au NPs (see Figure S3A-c in the Supporting Information). Iron oxide has no characteristic peak in the visible region (see Figure S3A-a in the Supporting Information). The red-shifted plasmonic absorption is attributed to the combination of Au NPs onto $\text{IP}_6\text{-Fe}_3\text{O}_4$ NPs. $\text{Fe}_3\text{O}_4/\text{Au}/\text{Ag}$ nanocomposites have a broad plasmon band at 400–410 nm, which is also red-shifted compared with the band at 398 nm of PA-Ag NPs (see Figure S3A-b in the Supporting Information). With increasing volume of 0.18 mg/mL Ag NPs from 1 to 4 mL, the Ag SPR band of the resultant $\text{Fe}_3\text{O}_4/\text{Au}/\text{Ag}$ nanocomposites becomes higher (Figure S3A-e–h in the Supporting Information). SERS measurements were conducted to observe the enhancement effect of the as-obtained nanocomposites using R6G molecule as a Raman probe (see Figure S3B in the Supporting Information) and the corresponding statistics of Raman peak intensity of R6G at 774 cm^{-1} was made (see Figure S3C in the Supporting Information). It demonstrated that $\text{Fe}_3\text{O}_4/\text{Au}/\text{Ag}$ nanocomposites made by addition of 3 mL of 0.18 mg mL^{-1} Ag NPs had the highest SERS activity. The molar ratio of Fe, Au, and Ag in the optimized $\text{Fe}_3\text{O}_4/\text{Au}/\text{Ag}$ -nanocomposites was about 6.62:1.00:1.07, determined by ICP-AES. SERS spectra of adenosine on Fe_3O_4 , $\text{Fe}_3\text{O}_4/\text{Au}$, and $\text{Fe}_3\text{O}_4/\text{Au}/\text{Ag}$ nanocomposites were performed (see Figure S4 in the Supporting Information). The binding forces between the nanocomposites and adenosine may be interaction of $-\text{NH}_2$ groups with Ag NPs and Au NPs through electrostatic attraction or coordination bonding.^{25,26} Ag NPs not only adsorb more adenosine molecules but Ag/Au NPs could also contribute to greater Raman enhancement.²³

Portable Raman Determination of Adenosine Using $\text{Fe}_3\text{O}_4/\text{Au}/\text{Ag}$ Nanocomposites. As above-mentioned, the determination of adenosine is usually performed using HPLC and GC-MS and time-consuming sample pretreatment methods such as solvent evaporation, cryogenic preconcentration, or stable isotopic labeling are needed. In this work, we do effort to explore the rapid and label-free analysis of adenosine in urine by $\text{Fe}_3\text{O}_4/\text{Au}/\text{Ag}$ nanocomposite-based SERS assay. Figure 2A is the concentration-dependent SERS spectra of adenosine in ultrapure water from 0.50 nM to 50 μM , measured by a micro-Raman system and $\text{Fe}_3\text{O}_4/\text{Au}/\text{Ag}$ nanocomposites concentrated by an extra magnetic field. Both Raman peaks at 743 and 972 cm^{-1} are from ring breathing modes of adenosine molecule. To meet the need of on-site analysis of adenosine in human urine, we used a portable Raman spectrometer to detect trace adenosine in ultrapure water. SERS spectra of aqueous adenosine at various concentrations were recorded by a portable Raman system under same experimental condition. In Figure 2B, the peak

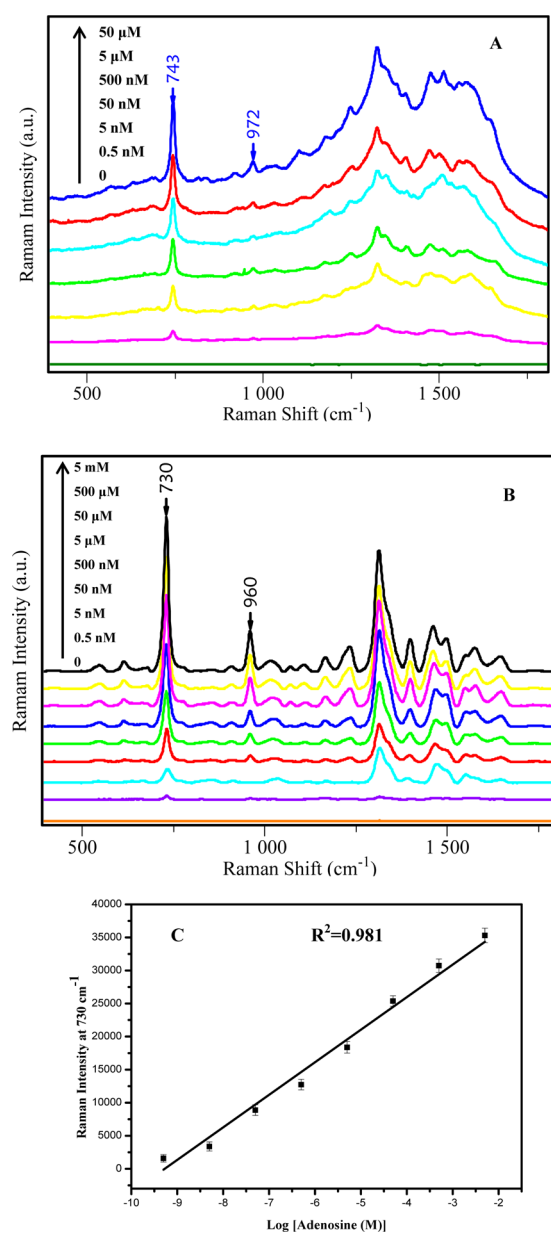


Figure 2. Concentration-dependent SERS spectra of aqueous adenosine recorded after mixed with $\text{Fe}_3\text{O}_4/\text{Au}/\text{Ag}$ nanocomposites (A) using confocal Raman (excitation laser at 633 nm) and (B) using a portable stabilized R. laser analyzer (excitation laser at 785 nm with a power of 300 mW). (C) Linear correlation of Raman intensities (at 730 cm^{-1}) with the logarithm of adenosine concentrations from 0.5 nM to 5 mM.

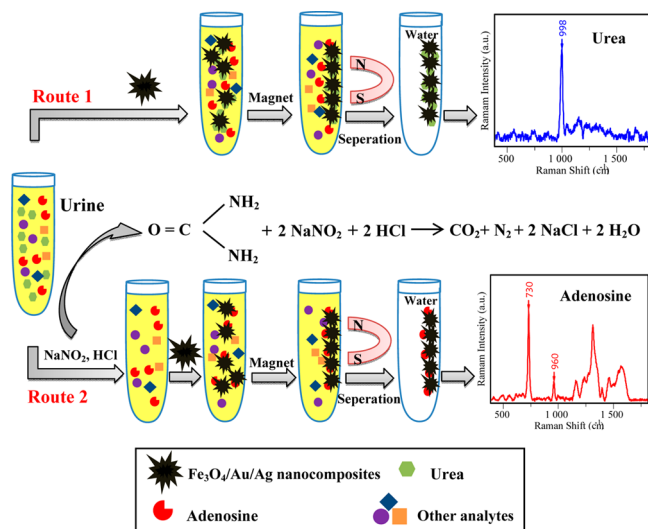
intensities at 730 and 960 cm^{-1} ascend with the increase in concentration of adenosine. Figure 2C is the linear relationship between the logarithm of aqueous adenosine concentrations from 0.5 nM to 5 mM and the SERS intensities at 730 cm^{-1} . Surprisingly, at the level of 0.5 nM, the Raman signals of adenosine at 730 and 960 cm^{-1} can be clearly seen, illustrating the high sensitivity of magnetically assisted SERS method for the detection of adenosine.

The interference of other nucleosides with the $\text{Fe}_3\text{O}_4/\text{Au}/\text{Ag}$ nanocomposites-based SERS detection of adenosine was investigated. Figure S5A–D in the Supporting Information is the SERS spectra of various concentrations of guanosine (characteristic Raman peaks at 661 and 961 cm^{-1}), cytidine

(characteristic Raman peaks at 784 and 1030 cm^{-1}), thymidine (characteristic Raman peaks at 788 cm^{-1}), and uridine (characteristic Raman peaks at 729, 777, and 960 cm^{-1}). In addition, the limit of detection (LOD) of guanosine, cytidine, thymidine, and uridine are of 50 nM, 5 nM, 500 μM , and 500 μM , respectively. It is found that uridine has a similar peak at 729 cm^{-1} compared with adenosine. The experimental results in Figure S6 in the Supporting Information showed that in spite of high concentrations, urea could not interfere with the adenosine assay. It can be clearly seen that characteristic peaks of adenosine (730 and 960 cm^{-1}) are visible and the Raman intensity at 730 cm^{-1} of adenosine is nearly unchangeable in the presence of high concentration of uridine (1 M). The possible reason is that uridine is difficult to bind with the surfaces of metal NPs without $-\text{NH}_2$ group in its molecule. When uridine and adenosine coexist in the solution, adenosine is preferably adsorbed on Au NPs or Ag NPs via $-\text{NH}_2$, occupying adsorption sites of surface. Adenosine has an apparently distinguishable band at 730 cm^{-1} through the observation of SERS spectra in Figure S5E in the Supporting Information and SERS results of adenosine with coexisting four equimolar nucleosides with all recoveries in the range of 95–105% given in Table S1 in the Supporting Information. Because of no contamination from other four nucleosides, the label-free $\text{Fe}_3\text{O}_4/\text{Au}/\text{Ag}$ nanocomposites-based SERS method is suitable for selectively determining adenosine. Consequently, $\text{Fe}_3\text{O}_4/\text{Au}/\text{Ag}$ nanocomposite-based SERS method could be developed as the sensitive, selective, and label-free protocol to detect the adenosine in urine.

Portable Raman Estimation of Adenosine in Human Urine. Human serum is a highly complex matrix including protein, which could severely interfere with the direct determination of adenosine (see Figure S7 in the Supporting Information). Human urine as an alternative sample consists of salts and small molecules, such as urea and nucleosides. As shown in Figure S8 in the Supporting Information, following the Route 1 of experimental strategies (Scheme 1) using $\text{Fe}_3\text{O}_4/\text{Au}/\text{Ag}$ -nanocomposite-based SERS protocol, the di-

Scheme 1. Schematic Presentation of Two Routes of Analytical Protocol: Route 1, Directly Detect Adenosine in Urine by SERS Technique; Route 2, Detect Adenosine in Urine by SERS Technique after Azo Coupling Reaction



rectly obtained spectra of healthy human urine (see Figure S8b in the Supporting Information) and healthy human urine spiked with 1 mM adenosine (see Figure S8a in the Supporting Information) are quite similar to the SERS spectrum of 0.3 M urea solution (see Figure S8c in the Supporting Information). The peak of urea at 998 cm^{-1} dominates in each SERS spectrum (see Figure S8 in the Supporting Information). Obviously, urea in urine seriously interfered with the SERS detection of adenosine. The strong adsorption of urea onto the silver and gold surfaces via $-\text{NH}_2$ groups impedes the adsorption of adenosine molecules in urine. Therefore, to remove the interference of urea was an urgent need. For this aim, the amount of urea in human urine was estimated first. Figure S9a in the Supporting Information shows the Raman spectra of urea in water with the concentrations increasing from 10 mM to 1 M. The linear relationship plotted by SERS intensities at 998 cm^{-1} and the urea concentrations is shown in Figure S9b in the Supporting Information. The concentration of urea in human urine was estimated to be 0.32 M, which was in accordance with the concentration of urea in human urine, 1.8% (0.3 M).²⁷

Azo coupling reaction could be employed to eliminate the urea. Urea reacted with HCl and NaNO_2 at low temperature and the azo products are mainly gas and NaCl , which is easy to be manipulated. In SERS spectrum of 0.3 M urea solution of Figure 3a, the peak at 998 cm^{-1} is from urea. After the addition

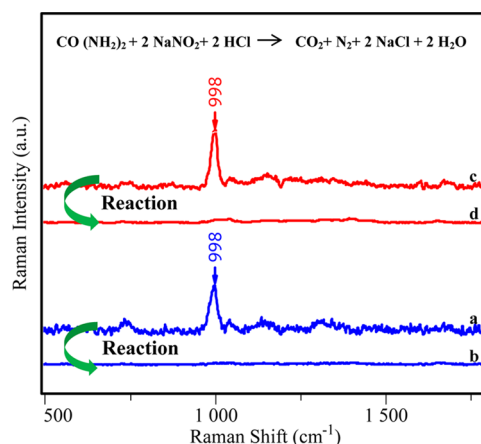


Figure 3. SERS spectra of aqueous urea (a) before and (b) after azo coupling reaction; SERS spectra of human urine (c) before and (d) after reaction.

of the same volume of HCl (0.6 M) and NaNO_2 (0.6 M) under ice-bath condition, the peak at 998 cm^{-1} disappears in SERS spectrum of Figure 3b. In Figure 3d, when human urine is treated with the azo coupling reaction, the peak of urea is also vanished. In addition, aqueous adenosine (1 μM) was conducted of azo coupling reaction based on the same experiment condition as urea. The SERS spectra of adenosine before and after azo coupling reaction are given in Figure S10 in the Supporting Information. Clearly, there is no effect of the azo coupling reaction on the Raman intensity of adenosine (730 cm^{-1}). Normally, high salt solution especially Cl^- , a product of azo coupling reaction, leads to the serious aggregation of nanocomposites^{28,29} and inaccurate SERS results. Figure S11A in the Supporting Information is the $\text{Fe}_3\text{O}_4/\text{Au}/\text{Ag}$ nanocomposite-based SERS spectra of 1 μM adenosine with the concentrations of NaCl from 0.01 to 1 M.

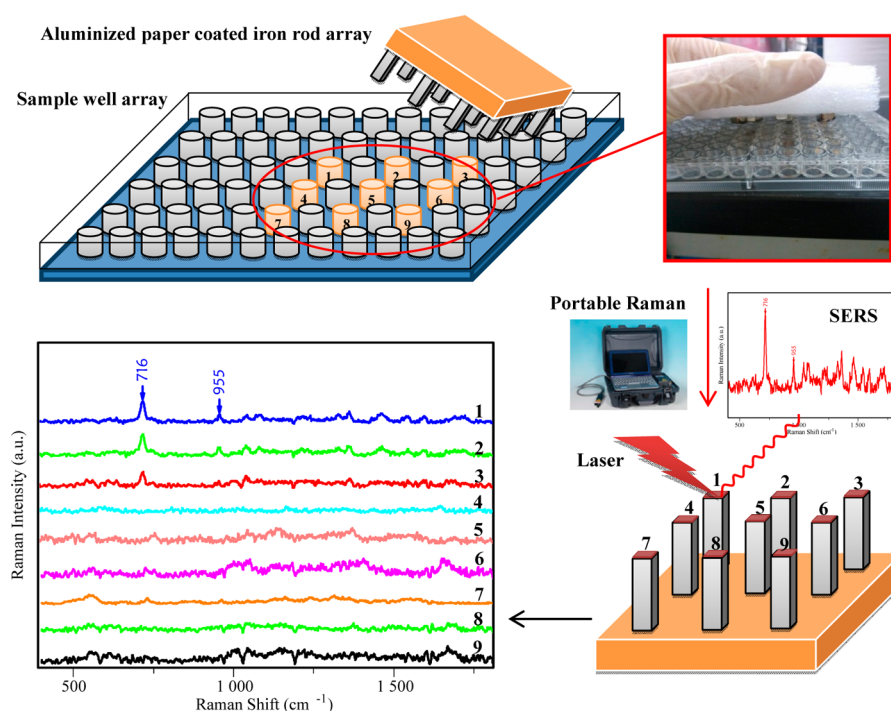


Figure 4. Array setup and procedures in the detection of adenosine in urine samples in a massive way by Fe₃O₄/Au/Ag nanocomposites with a portable Raman (inset is SERS spectra obtained on each rod from 1 to 9).

In Figure S11B in the Supporting Information, the statistic result of Raman intensities of adenosine at 730 cm⁻¹ and various concentrations of NaCl solutions illustrate no effect of high salt on the SERS measurement of adenosine. Clearly, the label-free Fe₃O₄/Au/Ag nanocomposite-based SERS method is quite robust for analytical application in high concentration of salt solution.

Before the real application, we first mimic the spiked human urine samples to evaluate the experimental procedure of Route 2 (Scheme 1). In detail, the spiked samples with different concentrations of adenosine were diluted 10-fold by water and then were treated by azo coupling reaction to eliminate urea. The pretreated samples sufficiently mixed with the due amount of Fe₃O₄/Au/Ag nanocomposites were accumulated by an external magnet to extract adenosine molecules from the physiological sample. The obtained Raman result is shown in Figure S12 in the Supporting Information. After the elimination of urea, the Raman peaks of adenosine at 730 and 960 cm⁻¹ are visible, and the LOD for adenosine in human urine can reach 0.1 μM. The same samples of spiked human urine were also analyzed using HPLC-MS (see Table S2 in the Supporting Information). The HPLC-MS experiments confirmed that Fe₃O₄/Au/Ag nanocomposite-based SERS protocol was validated to detect the trace adenosine in the spiked urine sample. In turn, compared with the HPLC, it is noteworthy that the newly developed label-free SERS method with selectivity and sensitivity is considerably faster, more economically advantageous, and easier to pretreat. Though the relative standard deviation for detecting adenosine in urine with the SERS method is nearly 9%, HPLC method usually requires massive standard derivatization and labeling to increase their selectivity and sensitivity for determining trace adenosine in urine but the removal of labeling and preconcentration steps leads to a poor LOD.

Under the optimized condition, the proposed SERS method was applied to analyze adenosine in human urine samples obtained from three preoperation patients of lung cancer. With the purpose of fast screening hundreds of samples, an array of tubes as the numerous chemical reactors and corresponding iron rod array coated with aluminized paper as parallel collectors were designed. Figure 4 gives a scheme of the SERS-array detection experiment. In detail, 100 μL of patients' urine was diluted 10-fold with water and then 5 μL of 5.4 mg/mL Fe₃O₄/Au/Ag nanocomposites were put into the each tube. After a diazotization process with adding 6 μL of 1 M NaNO₂ and 6 μL of 1 M HCl for 5 min at 4 °C, the aluminized paper coated iron rod array was dipped into the tubes for 3 min and taken out for collecting Fe₃O₄/Au/Ag nanocomposites. Finally, a portable Raman spectrometer was used to scan the top of nine iron rods to acquire the SERS spectra. After the SERS-array experiments, the aluminized paper could be conveniently changed for next detections. Inset of Figure 4 shows the corresponding SERS-array spectra of adenosine recorded from nine urine samples (samples 1–3 are from three lung cancer patients and samples 4–9 are from six health volunteers). As a result, in the samples of patient urine, the Raman peaks of adenosine at 716 and 955 cm⁻¹ are clearly visible, whereas no Raman peak of adenosine is seen in samples from 4 to 9. It should be mentioned that the Raman bands (716 and 955 cm⁻¹) of adenosine in urine samples were not consistent with these bands (730 and 960 cm⁻¹) of adenosine in water. The Raman bands (716 and 955 cm⁻¹) of adenosine in cancer patients' urine samples were detected after azo coupling reaction but the pretreated urine was still mixture, which might affect the adsorption fashion of adenosine. The band at 716 cm⁻¹ from purine ring indicates the adenosine adsorption via –NH₂ group,³⁰ which is similar to the Raman peak of 712 cm⁻¹ of powder adenosine sample (see Figure S13 in the Supporting Information). In the case of adenosine in water, it

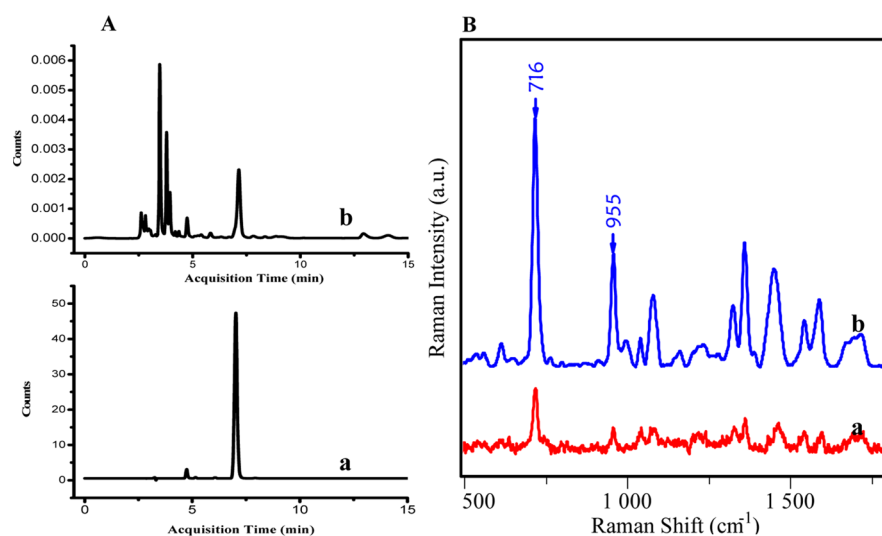


Figure 5. (A) SERS spectra of urine samples from lung cancer patient (a) before and (b) after spin steaming technology to concentrate urine. (B) HPLC-MS chromatograms of (a) 1 mM aqueous adenosine and (b) urine sample of a lung cancer patient after spin steaming technology.

anchored onto the metal surface via $-\text{NH}_2$ and N in imidazole ring, presenting a Raman band at 730 cm^{-1} .³¹

The HPLC-MS experiments were also performed for determining the adenosine in above three urine samples of patients. For HPLC-MS experiments, the samples needed to be concentrated for 100 times with spin steaming technology (SST) due to the trace adenosine in urine. A HPLC-MS result of aqueous adenosine as an example is shown in Figure 5A-a and its acquisition time is at 7.0 min. The corresponding HPLC-MS result of the urine sample of a patient after SST is given in Figure 5A-b illustrates the existence of adenosine in the cancer patient's urine. The results from the magnetically assisted SERS approach and the results from the HPLC method are tabulated in Table 1. All the results obtained are statistically

Table 1. Comparison of Real Detection of Adenosine in Lung Cancer Patients' Urine Using Magnetically Assisted SERS Protocol and HPLC-MS Assay

sample	gender	age (year)	SERS method $\bar{X} \pm \text{SD}$ (μM)	HPLC-MS $\bar{X} \pm \text{SD}$ (μM)	<i>t</i> value
1	male	62	76 ± 6	78 ± 4	0.82
2	male	58	32 ± 2	35 ± 2	
3	female	60	102 ± 5	112 ± 2	

analyzed using Student *t* test, and the Student's *t*-values at 95% confidence level do not exceed the theoretical values ($t_{0.05,8} = 2.306$), indicating no statistical difference between these two

analytical methods. Meanwhile, one of the samples of urine concentrated by SST was also detected with $\text{Fe}_3\text{O}_4/\text{Au}/\text{Ag}$ nanocomposite-based SERS protocol (Figure 5B-b) and its concentration of adenosine was estimated to be higher about 100-fold than that of no-processed urine (Figure 5A-a) by SST. The *Z'* factor of the SERS array detection is also calculated. Because $Z' = 0.90$, the SERS protocol is a good high-throughput screening method. The above investigation validates that the magnetically assisted SERS protocol as a strong alternative method has the merit to be applied in analysis of the clinical samples of urine for indicating the cancer.

In Table 2, the methods for adenosine detection in literature are summarized together with the first proposed Raman protocol for determining adenosine in human urine in this work. It should be noted that the experimental time of other non-SERS methods for one sample detection routinely costs more than 9 h, whereas the magnetically assisted SERS assay for one test is less than 20 min. Meanwhile, the label-free and simple SERS assay has a high sensitivity as same as the aptamer-based SERS methods.

The stability of $\text{Fe}_3\text{O}_4/\text{Au}/\text{Ag}$ nanocomposites-based SERS assay was assessed. First, SERS analysis of adenosine ($c = 1 \times 10^{-6}\text{ M}$) mixed with $\text{Fe}_3\text{O}_4/\text{Au}/\text{Ag}$ nanocomposites were continuously performed in the period of 8 months (see Figure S14 in the Supporting Information). Evidently, the monitoring SERS signals showed that the relative standard deviation among measured values was lower than 5%. We also evaluated the

Table 2. Comparison of Sensitivity for Adenosine Assay Methods

analytical method	label	LOD	calibration range	ref
electrochemical detection	label-free	0.1 μM	1 μM to 100 μM	32
electrochemical detection	label-free	1 nM	5 nM to 1 μM	33
chemiluminescence detection	label-free	80 nM	0.4 μM to 10 μM	34
SERS	label-free	0.5 nM	0.5 nM to 5 mM	this work
SERS	tetramethylrhodamine-labeled complementary ss-DNA	10 nM	20 nM to 2 μM	12
SERS	a triple helix aptamer	1.5 nM	5–500 nM	13
SERS	Au–Ag core–shell Ns-labeled aptamer	0.1 nM		14
colorimetric detection	AuNP-labeled aptamer	20 μM	20 μM to 2 mM	35
SPR	AuNP-tagged complementary ss-DNA	1 nM	1 nM to 1 μM	36

system stability of magnetically assisted SERS protocol. The spiked urine was treated by diazotization reaction and then mixed with Fe₃O₄/Au/Ag nanocomposites. SERS spectra of the above mixture consistently recorded within 10 days (see Figure S15 in the Supporting Information) revealed that the relative standard deviation (RSD) among respective intensities was lower than 5%.

CONCLUSION

Determination of adenosine as a possible biomarker for cancer is a demanding task. Herein, based on the synthesis of Fe₃O₄/Au/Ag nanocomposites, a magnetically assisted SERS protocol for fast analysis of trace adenosine level in lung cancer patients' urine was developed. The prepared Fe₃O₄/Au/Ag nanocomposites, which were connected and stabilized by phytic acid, exhibited a good stability and reproducibility. The magnetically assisted SERS protocol showed the merit of sensitivity, selectivity, simple pretreatment and rapid test. It could be applied as an on-site quantitative method when a portable Raman was used. It is noteworthy that azo coupling successfully removed urea in urine, which seriously interfered with the SERS signal of adenosine. Additionally, an array-tube-based SERS protocol was suggested for massive measurements of urine samples from patients. As a perspective, label-free Fe₃O₄/Au/Ag nanocomposite-based SERS protocol could be developed as a smart and promising system for the on-site effective assessments of human healthcare.

ASSOCIATED CONTENT

Supporting Information

XPS patterns, UV–visible spectra, and SERS spectra. This material is available free of charge via the Internet at <http://pubs.acs.org>.

AUTHOR INFORMATION

Corresponding Author

*E-mail: haifengyang@yahoo.com. Telephone: +86-21-64321701.

Notes

The authors declare no competing financial interest.

ACKNOWLEDGMENTS

This work is supported by the National Natural Science Foundation of China (21475088), PCSIRT (IRT1269) and International Joint Laboratory on Resource Chemistry (IJLRC). We also express many thanks for the help of Dr. Yang Sun in Shanghai Tongji Hospital and Shanghai Pulmonary Hospital for providing the urine samples.

REFERENCES

- (1) Hu, P.; Zhu, C.; Jin, L.; Dong, S. An Ultrasensitive Fluorescent Aptasensor for Adenosine Detection Based on Exonuclease III Assisted Signal Amplification. *Biosens. Bioelectron.* **2012**, *34*, 83–87.
- (2) Sachdeva, S.; Gupta, M. Adenosine and Its Receptors as Therapeutic Targets: An Overview. *Saudi Pharm. J.* **2013**, *21*, 245–253.
- (3) Zhang, J. Q.; Wang, Y. S.; He, Y.; Jiang, T.; Yang, H. M.; Tan, X.; Kang, R. H.; Yuan, Y. K.; Shi, L. F. Determination of Urinary Adenosine using Resonance Light Scattering of Gold Nanoparticles Modified Structure-Switching Aptamer. *Anal. Biochem.* **2010**, *397*, 212–217.

- (4) Swamy, B. E. K.; Venton, B. J. Subsecond Detection of Physiological Adenosine Concentrations Using Fast-Scan Cyclic Voltammetry. *Anal. Chem.* **2007**, *79*, 744–750.

- (5) Taniai, H.; Sumi, S.; Ito, T.; Ueta, A.; Ohkubo, Y.; Togari, H. A Simple Quantitative Assay for Urinary Adenosine Using Column-Switching High-Performance Liquid Chromatography. *Tohoku J. Exp. Med.* **2006**, *208*, 57–63.

- (6) Liebich, H. M.; Stefano, C. D.; Wixforth, A.; Schmid, H. R. Quantitation of Urinary Nucleosides by High-Performance Liquid Chromatography. *J. Chromatogr. A* **1997**, *763*, 193–197.

- (7) Langridge, J. I.; McClure, T. D.; Ei-Shakawi, S.; Fielding, A.; Schram, K. H.; Newton, R. P. Gas chromatography/Mass Spectrometric Analysis of Urinary Nucleosides in Cancer Patients; Potential of Modified Nucleosides as Tumour Markers. *Rapid Commun. Mass Spectrom.* **1993**, *7*, 427–434.

- (8) Nie, S.; Emory, S. R. Probing Single Molecules and Single Nanoparticles by Surface-Enhanced Raman Scattering. *Science* **1997**, *275*, 1102–1106.

- (9) Michaels, A. M.; Nirmal, M.; Brus, L. E. Surface Enhanced Raman Spectroscopy of Individual Rhodamine 6G Molecules on Large Ag Nanocrystals. *J. Am. Chem. Soc.* **1999**, *121*, 9932–9939.

- (10) Kneipp, J.; Kneipp, H.; Kneipp, K. SERS-A Single-Molecule and Nanoscale Tool for Bioanalytics. *Chem. Soc. Rev.* **2008**, *37*, 1052–1060.

- (11) Dasary, S. S. R.; Singh, A. K.; Senapati, D.; Yu, H.; Ray, P. C. Gold Nanoparticle Based Label-Free SERS Probe for Ultrasensitive and Selective Detection of Trinitrotoluene. *J. Am. Chem. Soc.* **2009**, *131*, 13806–13812.

- (12) Chen, J. W.; Liu, X. P.; Feng, K. J.; Liang, Y.; Jiang, J. H.; Shen, G. L.; Yu, R. Q. Detection of Adenosine Using Surface-Enhanced Raman Scattering Based on Structure-Switching Signaling Aptamer. *Biosens. Bioelectron.* **2008**, *24*, 66–71.

- (13) Zheng, J.; Hu, Y.; Bai, J.; Ma, C.; Li, J.; Li, Y.; Shi, M.; Tan, W.; Yang, R. Universal Surface-Enhanced Raman Scattering Amplification Detector for Ultrasensitive Detection of Multiple Target Analytes. *Anal. Chem.* **2014**, *86*, 2205–2212.

- (14) Chang, Y. C.; Ko, F. H. Aptamer Based Surface Enhanced Raman Scattering Detection of Adenosine Using Various Core Sizes of Au–Ag Core–Shell Nanoparticles. *RSC Adv.* **2014**, *4*, 26251–26257.

- (15) Yang, Y.; Liu, J.; Fu, Z. W.; Qin, D. Galvanic Replacement-Free Deposition of Au on Ag for Core–Shell Nanocubes with Enhanced Chemical Stability and SERS Activity. *J. Am. Chem. Soc.* **2014**, *136*, 8153–8156.

- (16) Bai, T.; Sun, J.; Che, R.; Xu, L.; Yin, C.; Guo, Z.; Gu, N. Controllable Preparation of Core–Shell Au–Ag Nanoshuttles with Improved Refractive Index Sensitivity and SERS Activity. *ACS Appl. Mater. Interfaces* **2014**, *6*, 3331–3340.

- (17) Saha, A.; Jana, N. R. Detection of Cellular Glutathione and Oxidized Glutathione Using Magnetic–Plasmonic Nanocomposite-Based “Turn-Off” Surface Enhanced Raman Scattering. *Anal. Chem.* **2013**, *85*, 9221–9228.

- (18) Shen, J.; Zhu, Y.; Yang, X.; Zong, J.; Li, C. Multifunctional Fe₃O₄@Ag/SiO₂/Au Core–Shell Microspheres as a Novel SERS-Activity Label via Long-Range Plasmon Coupling. *Langmuir* **2013**, *29*, 690–695.

- (19) Ranc, V.; Markova, Z.; Hajdich, M.; Prucek, R.; Kvitik, L.; Kaslik, J.; Safarova, K.; Zboril, R. Magnetically Assisted Surface-Enhanced Raman Scattering Selective Determination of Dopamine in an Artificial Cerebrospinal Fluid and a Mouse Striatum Using Fe₃O₄/Ag Nanocomposite. *Anal. Chem.* **2014**, *86*, 2939–2946.

- (20) Han, X. X.; Chen, L.; Kuhlmann, U.; Schulz, C.; Weidinger, I. M.; Hildebrandt, P. Magnetic Titanium Dioxide Nanocomposites for Surface-Enhanced Resonance Raman Spectroscopic Determination and Degradation of Toxic Anilines and Phenols. *Angew. Chem., Int. Ed.* **2014**, *53*, 2481–2484.

- (21) Ding, Q.; Ma, Y.; Ye, Y.; Yang, L.; Liu, J. A Simple Method to Prepare the Magnetic Ni@Au Core-Shell Nanostructure for the Cycle Surface Enhanced Raman Scattering Substrates. *J. Raman Spectrosc.* **2013**, *44*, 987–993.

(22) Yang, T.; Guo, X.; Wang, H.; Fu, S.; Yu, J.; Wen, Y.; Yang, H. Au Dotted Magnetic Network Nanostructure and Its Application for On-Site Monitoring Femtomolar Level Pesticide. *Small* **2014**, *10*, 1325–1331.

(23) Chang, H.; Kang, H.; Yang, J. K.; Jo, A.; Lee, H. Y.; Lee, Y. S.; Jeong, D. H. Ag Shell–Au Satellite Hetero-Nanostructure for Ultra-Sensitive, Reproducible, and Homogeneous NIR SERS Activity. *ACS Appl. Mater. Interfaces* **2014**, *6*, 11859–11863.

(24) Tan, C. J.; Chua, H. G.; Ker, K. H.; Tong, Y. W. Preparation of Bovine Serum Albumin Surface-Imprinted Submicrometer Particles with Magnetic Susceptibility through Core-Shell Miniemulsion Polymerization. *Anal. Chem.* **2008**, *80*, 683–692.

(25) Kumar, A.; Mandal, S.; Selvakannan, P. R.; Pasricha, R.; Mandale, A. B.; Sastry, M. Investigation into the Interaction between Surface-Bound Alkylamines and Gold Nanoparticles. *Langmuir* **2003**, *19*, 6277–6282.

(26) Hussain, J. I.; Kumar, S.; Hashmi, A. A.; Khan, Z. Silver Nanoparticles: Preparation, Characterization, and Kinetics. *Adv. Mater. Lett.* **2011**, *2*, 188–194.

(27) Marshall, E. K. A Rapid Clinical Method for the Estimation of Urea in Urine. *J. Biol. Chem.* **1913**, *14*, 283–290.

(28) Doctor, E. L.; McCord, B. Comparison of Aggregating Agents for the Surface-Enhanced Raman Analysis of Benzodiazepines. *Analyst* **2013**, *138*, 5926–5932.

(29) Han, S.; Hong, S.; Li, X. Effects of Cations and Anions as Aggregating Agents on SERS Detection of Cotinine (COT) and Trans-3'-Hydroxycotinine (3HC). *J. Colloid Interface Sci.* **2013**, *410*, 74–80.

(30) Yang, H.; Yang, Y.; Liu, Z.; Zhang, Z.; Shen, G.; Yu, R. Self-Assembled Monolayer of NAD at Silver Surface: A Raman Mapping Study. *Surf. Sci.* **2004**, *551*, 1–8.

(31) Taniguchi, I.; Umekita, K.; Yasukouchi, K. Surface-Enhanced Raman Scattering of Nicotinamide Adenine Dinucleotide (NAD⁺) Adsorbed on Silver and Gold Electrodes. *J. Electroanal. Chem.* **1986**, *202*, 315–322.

(32) Li, B.; Du, Y.; Wei, H.; Dong, S. Reusable, Label-free Electrochemical Aptasensor for Sensitive Detection of Small Molecules. *Chem. Commun.* **2007**, *36*, 3780–3782.

(33) Feng, K.; Sun, C.; Kang, Y.; Chen, J.; Jiang, J. H.; Shen, G. L.; Yu, R. Q. Label-free Electrochemical Detection of Nanomolar Adenosine Based on Target-Induced Aptamer Displacement. *Electrochem. Commun.* **2008**, *10*, 531–535.

(34) Yan, X.; Cao, Z.; Kai, M.; Lu, J. Label-Free Aptamer-Based Chemiluminescence Detection of Adenosine. *Talanta* **2009**, *79*, 383–387.

(35) Zhao, W.; Chiuman, W.; Lam, J. C. F.; McManus, S. A.; Chen, W.; Cui, Y.; Pelton, R.; Brook, M. A.; Li, Y. DNA Aptamer Folding on Gold Nanoparticles: From Colloid Chemistry to Biosensors. *J. Am. Chem. Soc.* **2008**, *130*, 3610–3618.

(36) Wang, J.; Zhou, H. S. Aptamer-Based Au Nanoparticles-Enhanced Surface Plasmon Resonance Detection of Small Molecules. *Anal. Chem.* **2008**, *80*, 7174–7178.